Investigation of impurity tracer transport in high density plasmas at the stellarator Wendelstein 7-AS

R. Burhenn, M.Anton, J. Baldzuhn, R. Brakel, L. Giannone, H. Hacker, M. Hirsch, L. Ledl, M. Maassberg, U. Stroth, A. Weller,
W7-AS Team, ECRH Group[1], NI Group
Max-Planck-Institut für Plasmaphysik, EURATOM Ass., D-85748 Garching, FRG
[1]Institut für Plasmaforschung, Universität Stuttgart, D-70569 Stuttgart, FRG

Introduction - For the decay time of injected tracer impurities (aluminum laser blow-off) in W7-AS, the electron density is, among others, an important scaling parameter [1], indicating improved confinement of impurities towards high electron density. Previous impurity injection experiments (H_2S gas oscillation and Al laser blow-off) [1] at medium density (n_{e0}=2-5·10^{19} m^{-3}) could partially be simulated within the errors by the one-dimensional radiation and transport code SITAR [2], based on neoclassical and Pfirsch-Schlüter transport for axisymmetric devices. At low density, the transport was found to be significantly higher than predicted, whereas at high density (n_{e0}=6.5·10^{19} m^{-3}), the neoclassical fluxes had to be reduced to fit the experimental data. Analysis of further discharges at different electron densities, using a simple transport model (diffusion coefficient D(r)=const, inward velocity $v(r)=(r/a)v_{(r=a)}$, a: plasma radius), supports the trend of decreased diffusion coefficients towards higher density, which cannot be attributed simply to a decrease in Z_{eff}. A similar dependence of D on electron density was already observed in ECF heated Heliotron E plasmas [3] and supposed to be caused by changes in D rather than in the flow velocity, the latter being close to the classical expectations. In order to elucidate the density dependence in W7-AS, discharges with densities varied by a factor of 2 (n_{e0}=3.5/7·10^{19} m^{-3}) are analyzed in more detail (fig.1), together with fluctuation- and MHD-diagnostics and measurement of the radial electric field. Especially in non-axisymmetric devices like stellarators, the latter can play an important role for impurity transport [4], but is not yet included in SITAR.

Simulations with simple assumptions about D(r)- and v(r)-profiles might mask possible local changes in transport. Therefore, the radial transport coefficients were tried to be directly derived from the temporal and radial behaviour of spectral radiation, detected by the SX-camera during the penetration process of injected aluminum by laser blow-off. Indications were expected, whether the modification of the transport coefficients happens in the core plasma or somewhere in the plasma boundary.

Transport analysis - Because of its good radial and temporal resolution, the SX-camera is a proper diagnostic tool at W7-AS for transport investigation. In spite of its energy-integrated information, the use of a 25µm Be-filter in front of the camera offers the possibility to restrict the number of ionization states contributing to the measured intensity and simplifies the reconstruction of the total impurity density profiles. For total impurity density reconstruction during the penetration process of injected aluminum, the radial intensity profile at each time-step was abel-inverted (figs.1b,e) and converted to a total impurity density profile assuming coronal equilibrium (quasi-stationary condition) in a first step. This is considered to be applicable in

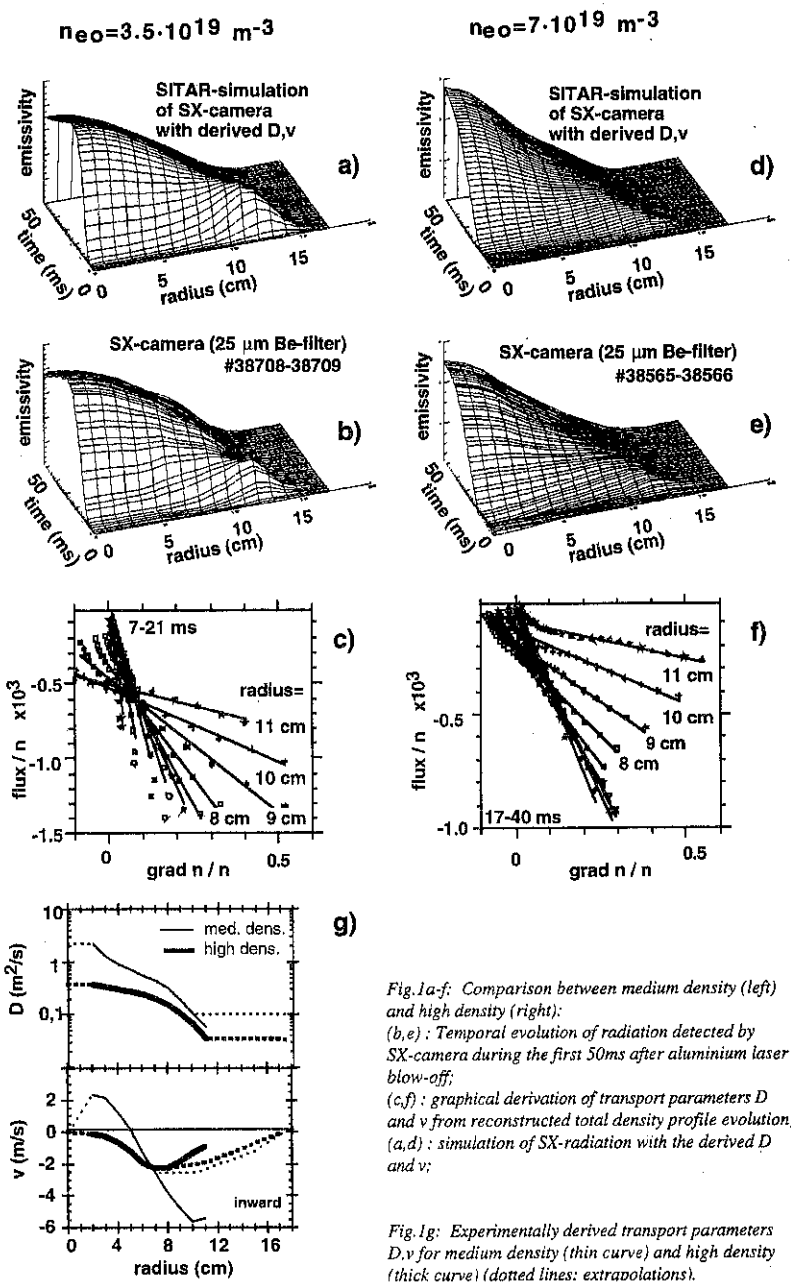

Fig.1a-f: Comparison between medium density (left) and high density (right):
(b,e) : Temporal evolution of radiation detected by SX-camera during the first 50ms after aluminium laser blow-off;
(c,f) : graphical derivation of transport parameters D and v from reconstructed total density profile evolution;
(a,d) : simulation of SX-radiation with the derived D and v;

Fig.1g: Experimentally derived transport parameters D,v for medium density (thin curve) and high density (thick curve) (dotted lines: extrapolations).

low-transport discharges at high electron density. The transport coefficients at a certain radial position can then be derived from the local temporal evolution of the total impurity density profiles n(r,t) [5]. With the ansatz Γ=-D grad(n)+vn, D and v can be determined by fitting a straight line, when plotting the normalized total impurity fluxes Γ/n vs. the normalized total density gradients grad(n)/n for all time points at this radial position (figs.1c,f). The flux Γ can be estimated from the density profile evolution using the continuity equation dn/dt=-div(Γ) with restriction to radial regions where external sources and sinks can be neglected.

In cases where the assumption of quasi-stationarity might not hold, the reconstruction with coronal equilibrium can cause errors. Therefore, the radial density profiles for each time step were reconstructed again, now using a reconstruction factor ß(r,t)=n(r,t)/P(r,t) (P:total local emissivity contributing to SX-camera) obtained from a transport and radiation calculation with SITAR, using the D- and v-values derived in the first step as input. A repeated derivation procedure for D and v, but now with the corrected density profile evolution as described above provides new transport coefficients (fig.1g) which, in fact, fit the SX-camera better in most cases (fig.1a,d). The accuracy of this iterative method strongly relies on the quality of abel-inversion and atomic data base. Possible errors have to be discussed in this context.

Results and discussion - In order to study the density dependence of impurity confinement at W7-AS, ECF-heated discharges (P_{ECF}=400kW) at two different densities (figs.1a,b,c: $n_{e0}=3.5\cdot10^{19}$ m^{-3}; figs.1d,e,f: $n_{e0}=7\cdot10^{19}$ m^{-3}) were compared. The transport coefficients were derived according to the procedure described above and are plotted in fig.1g for both densities.

For the outer plasma region, the last reliably determined value of the diffusion coefficients at r=10-11cm were kept constant up to the plasma edge. They represent average diffusion coefficients for this region, determining essentially the central time behaviour during the inflow phase. The extrapolated average diffusion coefficient for medium density approaches values consistent with neoclassically predicted ones (0.09m^2/s≥D≥0.04m^2/s, 10cm≥r≥17cm), but falls below the predictions (0.2m^2/s≥D≥0.07m^2/s, 10cm≥r≥17cm) for the high density case. This trend is even more pronounced at higher electron densities of $n_{e0}=1.2\cdot10^{20}$m^{-3}, e.g. in high confinement neutral-beam heated discharges [6], where transport coefficients were derived (D(r)=0.07m^2/s, v(r)=5m/s·(r/a), #38551), being clearly smaller than predicted by SITAR, in which the fluxes are already reduced by 50% to account for the W7-AS transport optimization.

The convection velocity was extrapolated to vanish in the plasma center and was adjusted in the outer part to fit better the temporal decay of spectral line intensities from different ionization states of aluminum, observed by central-line-of-sight crystal- and VUV-spectrometers (fig.2). For the high density discharge, only a slight correction in the derived v (fig.1g) was necessary to excellently fit all experimental data. In the case of medium density, D(r=10cm) was used for extrapolation and v has to be reduced by a factor of 2 for a good compromise in fitting the experimental data radially as well as temporally. A reduction of D in the outer region down to the value D(r=11cm) would fit the time traces of the spectrometers only for the case of vanishing convection velocity, but will lead to a misfit of the radial profiles.

In the two ECF-heated discharges under investigation, no substantial changes as well in the radial electric field E_r (within the error) as in MHD-activity and electron density profile shape

could be observed from which the difference in transport can be deduced. However, previous measurements of the density fluctuation level as a function of electron density [7] show some inverse dependence, but an effect on the impurity transport cannot simply be concluded.

In the case of high electron density, D is overall lower by a factor of 2-3 compared to the medium density discharge, v being quite similar. The resulting difference in confinement can be illustrated quite impressively by the change in decay time for the injected aluminium (fig.2). Consequently, also the time evolution of intrinsic impurity radiation and Z_{eff} is remarkably different during the flat-top phase for this two densities (fig.3). However, assuming a constant impurity influx of, e.g. intrinsic chlorine from the walls and using just the derived set of transport parameters, the difference in the time traces of Cl-XIV can be qualitatively well described (fig 3, fits): compared to medium electron density, where stationary conditions were achieved well within the pulse length (fig.3 curve b, arrow) due to higher transport, the reduced transport in the high density case causes longer times to establish stationarity (fig.3 curve a).

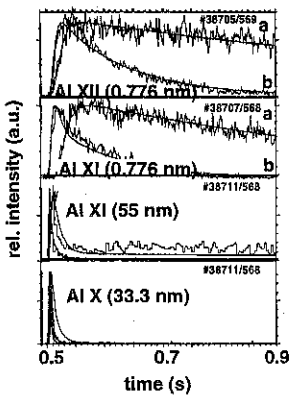

Fig.2: Time traces of spectral lines from different ionization states of aluminum fter injection by laser blow-off: (a) n_{eo}=7·0^{19}m^{-3}, (b) n_{eo}=3.5·10^{19} m^{-3}

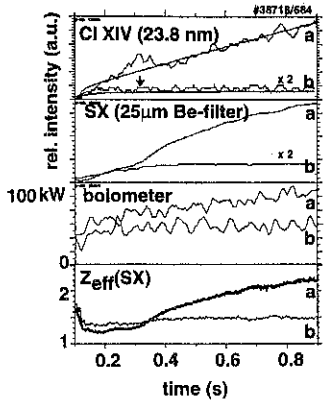

Fig.3: Temporal evolution of impurity radiation and Z_{eff}(SX) for (a) n_{eo}=7·10^{19}m^{-3}, (b) n_{eo}=3.5·10^{19} m^{-3} and simulations for Cl-XIV.

Similar behaviour for other intrinsic impurity species might explain the signals of the SX-camera, the bolometer and Z_{eff}. Nevertheless, at high density (n_{eo}=7·10^{19}m^{-3}) the extrapolated total radiation (bolometer) at the time when the Cl-XIV radiation should reach 90% of its stationary level (approx. at 1.7s, from simulation), stays well below the critical value of 60% of the heating power [8], where the plasma is severely affected by radiation.

References

[1] R.Burhenn et al., 22nd EPS Conf. on Contr. Fus. and Plasma Physics, Vol.19C, part III, p.145-148, Bournemouth 1995
[2] WVII-A Team, NI Group, Nucl. Fusion 25(11) 1593 (1985)
[3] H.Kaneko et al., Nucl. Fusion 27(7) 1075 (1987)
[4] A.Baldzuhn et al., this conference
[5] A.Weller et al., Plasma Physics and Controlled Fusion 33(13) (1991),1559
[6] U.Stroth et al., this conference
[7] U.Stroth, Report IPPIII/216
[8] P.Grigull et al., this conference